

Article

# Low-Energy Electron Elastic Collisions with Actinide Atoms Am, Cm, Bk, Es, No and Lr: Negative-Ion Formation

Alfred Z. Msezane \*  and Zineb Felfli

Department of Physics and CTSPS, Clark Atlanta University, Atlanta, GA 30314, USA; zfelfli@cau.edu

\* Correspondence: amsezane@cau.edu

**Abstract:** The rigorous Regge-pole method is used to investigate negative-ion formation in actinide atoms through electron elastic total cross sections (TCSs) calculation. The TCSs are found to be characterized generally by negative-ion formations, shape resonances and Ramsauer-Townsend (R-T) minima, and they exhibit both atomic and fullerene molecular behavior near the threshold. Additionally, a polarization-induced metastable cross section with a deep R-T minimum is identified near the threshold in the Am, Cm and Bk TCSs, which flips over to a shape resonance appearing very close to the threshold in the TCSs for Es, No and Lr. We attribute these new manifestations to size effects and orbital collapse significantly impacting the polarization interaction. From the TCSs unambiguous and reliable ground, metastable and excited states negative-ion binding energies (BEs) for Am<sup>-</sup>, Cm<sup>-</sup>, Bk<sup>-</sup>, Es<sup>-</sup>, No<sup>-</sup> and Lr<sup>-</sup> anions formed during the collisions are extracted and compared with existing electron affinities (EAs) of the atoms. The novelty of the Regge-pole approach is in the extraction of the negative-ion BEs from the TCSs. We conclude that the existing theoretical EAs of the actinide atoms and the recently measured EA of Th correspond to excited anionic BEs.

**Keywords:** generalized bound states; actinide atoms; elastic cross sections; anionic binding energies; electron correlations; core-polarization interaction; Regge poles

**PACS Nos:** 34.80. Bm; electron elastic scattering



**Citation:** Msezane, A.Z.; Felfli, Z. Low-Energy Electron Elastic Collisions with Actinide Atoms Am, Cm, Bk, Es, No and Lr: Negative-Ion Formation. *Atoms* **2021**, *9*, 84. <https://doi.org/10.3390/atoms9040084>

Academic Editor: Luca Argenti

Received: 12 August 2021

Accepted: 23 September 2021

Published: 19 October 2021

**Publisher's Note:** MDPI stays neutral with regard to jurisdictional claims in published maps and institutional affiliations.



**Copyright:** © 2021 by the authors. Licensee MDPI, Basel, Switzerland. This article is an open access article distributed under the terms and conditions of the Creative Commons Attribution (CC BY) license (<https://creativecommons.org/licenses/by/4.0/>).

## 1. Introduction

The determination of unambiguous and reliable values of electron affinities (EAs) for complex electron-heavy systems such as lanthanide and actinide atoms, as well as fullerene molecules, is currently one of the most challenging problems in atomic and molecular physics and still plagues both experiments and theories alike. Unfortunately, progress toward a theoretical understanding of the fundamental mechanisms underlying low-energy electron scattering from complex heavy atoms, including fullerene molecules, to stable, negative-ion formation has been very slow. Accurate and reliable atomic and molecular affinities are essential for understanding chemical reactions involving negative ions [1]. Additionally, the EA provides a stringent test of theoretical calculations when their results are compared with those from reliable measurements.

For most of the lanthanide atoms, producing sufficient anions that can be used in photodetachment experiments is very challenging [2]. For the actinide atoms the situation is even worse; due to their radioactive nature, they are difficult to handle experimentally. A great motivation for this investigation is the remarkable agreement between the recent first ever EA measurement of the highly radioactive At atom [3] and various theoretical EAs [4]. The authors of [3] used the coupled-cluster method, while [4] employed a multiconfiguration Dirac Hartree-Fock method. Furthermore, in [4], an extensive comparison among various sophisticated theoretical EAs was carried out. Most importantly, in the context of the present investigation, the measured EA of the atomic At matched excellently with the Regge-pole-calculated binding energy (BE) of the ground state of the At<sup>-</sup> anion (see Table 1

for the comparison). Additionally, recently the EAs of Th and Hf were measured [5,6]. For both atoms the measured and calculated EAs corresponded to the Regge-pole-calculated BEs of their anions in excited states [7,8] and not in their ground states.

Theoretically, the large number of electrons involved and the presence of open d- and f-electrons in both the lanthanide and actinide atoms, results in enormously intricate and diverse electron configurations. These present formidable computational complexities when using conventional theoretical methods, such as the Relativistic Configuration Interaction (RCI) method. This renders obtaining unambiguous and reliable EAs for these systems very difficult, if not impossible. Indeed, many existing experimental and sophisticated theoretical EAs of the lanthanides and actinides are difficult to interpret, see for example [7–10]. A serious question then arises: Does the EA of complex heavy systems correspond to the BE of electron attachment in the ground, metastable or the excited state of the formed negative ion during the collision?

The main objective of this paper is to investigate negative-ion formation in low-energy,  $E < 10$  eV, electron elastic scattering from the large actinide atoms, Am, Cm, Bk, Es, No and Lr, through the total cross sections (TCSs) calculation, and present new TCSs. From the TCSs, the unambiguous and reliable ground, metastable and excited-state, negative-ion binding energies (BEs) of the  $\text{Am}^-$ ,  $\text{Cm}^-$ ,  $\text{Bk}^-$ ,  $\text{Es}^-$ ,  $\text{No}^-$  and  $\text{Lr}^-$  anions, formed during the collisions, are extracted and compared with the existing EAs of these actinide atoms to understand the existing EAs. Additionally, we investigate in the TCSs of the atoms, Am to Lr, new manifestations due to the size effect and the effect of 6d-orbital collapse.

For the investigation we use the rigorous Regge pole method. The novelty and generality of the Regge-pole approach is in the extraction of the anionic BEs from the calculated TCSs of the complex heavy systems; for ground state collisions these BEs yield the unambiguous and definitive EAs, which are theoretically challenging to calculate. Very recently, the ground state anionic BEs extracted from our Regge-pole calculated electron elastic TCSs for the fullerene molecules,  $\text{C}_{20}$  through  $\text{C}_{92}$ , have been found to match excellently with the measured EAs (see [11,12] for comparison). For the complex, heavy atoms, Au and Pt, including the highly radioactive At, the agreement between our Regge-pole calculated ground-state anionic BEs and the measured EAs of Au [13–15], Pt [13,16,17] and At [3], as well as of  $\text{C}_{60}$  [18,19], is outstanding. The method requires no assistance whatsoever from either experiment or from any other theory to achieve the remarkable feat, namely obtaining the ground state anionic BEs for Au, Pt, and At atoms and the fullerene molecules,  $\text{C}_{20}$  through  $\text{C}_{92}$  [11,12], that match excellently with the measured EAs, see Table 1 for comparison.

The paper is organized as follows: Section 2 presents the Method of Calculation, Section 3 presents the Results and the Summary and Conclusions are presented in Section 4.

## 2. Method of Calculation

### 2.1. Elastic Scattering Total Cross Section (TCS)

The use of theoretical methods, that account adequately for the vital electron–electron correlation effects and core–polarization interaction, is fundamental to a reliable investigation and understanding of negative-ion formation in complex electron heavy systems. Regge poles, singularities of the S-matrix, rigorously define resonances [20,21] and in the physical sheets of the complex plane they correspond to bound states [22]. Being generalized bound states within the complex angular momentum (CAM) description of scattering, Regge poles are therefore appropriate for the present investigation. Indeed, in [23], it was confirmed that Regge poles formed during low-energy electron elastic scattering become stable bound states. In the Regge pole, also known as the CAM method, the important and revealing energy-dependent Regge trajectories are also calculated. Their effective use in low-energy electron scattering has been demonstrated in [24,25].

The Mulholland formula [26] is used here to calculate the near-threshold electron–atom/fullerene collision TCS, resulting in the formation of negative-ions as resonances.

In the formula below, the TCS fully embeds the essential electron–electron correlation effects [27,28] (atomic units are used throughout):

$$\sigma_{tot}(E) = 4\pi k^{-2} \int_0^\infty \text{Re}[1 - S(\lambda)] \lambda d\lambda - 8\pi^2 k^{-2} \sum_n \text{Im} \frac{\lambda_n \rho_n}{1 + \exp(-2\pi i \lambda_n)} + I(E) \quad (1)$$

In Equation (1),  $S(\lambda)$  is the S-matrix,  $k = \sqrt{2mE}$ , with  $m$  being the mass,  $E$  is the impact energy,  $\rho_n$  is the residue of the S-matrix at the  $n^{\text{th}}$  pole,  $\lambda_n$  and  $I(E)$  contains the contributions from the integrals along the imaginary  $\lambda$ -axis ( $\lambda$  is the complex angular momentum); its contribution is negligible [24].

## 2.2. The Potential

As in [29], here we consider the incident electron to interact with the neutral, complex and heavy system (atom/fullerene) without consideration of the complicated details of the electronic structure of the system itself. Therefore, within the Thomas–Fermi theory, Felfli et al. [30] generated the robust Avdonina–Belov–Felfli (ABF) potential which embedded the vital core–polarization interaction:

$$U(r) = -\frac{Z}{r(1 + \alpha Z^{1/3}r)(1 + \beta Z^{2/3}r^2)} \quad (2)$$

In Equation (2),  $Z$  is the nuclear charge,  $\alpha$  and  $\beta$  are variation parameters. For small  $r$ , the potential describes the Coulomb attraction between an electron and a nucleus,  $U(r) \sim -Z/r$ , while at large distances it has the appropriate asymptotic behavior, viz.  $\sim -1/(\alpha\beta r^4)$ , and properly accounts for the polarization interaction at low energies. For an electron, the source of the bound states giving rise to Regge trajectories is the attractive Coulomb well it experiences near the nucleus. By adding the centrifugal term to the well one could ‘squeeze’ these states into the continuum.

The strength of this extensively studied potential [31–33] lies in that it has five turning points and four poles connected by four cuts in the complex plane and can be continued analytically in the complex plan. The presence of the powers of  $Z$  as coefficients of  $r$  and  $r^2$  in Equation (2) ensures that the spherical and non-spherical atoms and fullerenes are correctly treated. Additionally, small and large systems are appropriately treated. The effective potential  $V(r) = U(r) + \lambda(\lambda + 1)/2r^2$  is considered here as a continuous function of the variables  $r$  and complex  $\lambda$ . The details of the numerical evaluations of the TCSs are described in [28] and further details of the calculations are found in [34].

The novelty and generality of the robust Regge-pole approach lies in that the crucial electron–electron correlation effects are fully embedded in the Mulholland formula. Additionally, the ABF potential contains the vital core–polarization interaction. These two important effects are identified as the major physical effects mostly responsible for electron attachment in low-energy electron scattering from complex heavy systems, leading to stable negative-ion formation. These effects are particularly important in the study of the experimentally difficult-to-handle radioactive actinide atoms, and because of the difficulty experienced by conventional theoretical calculations to obtain unambiguous and reliable EAs for the lanthanide and actinide atoms [7–9,35]. Crucial in the CAM methods are the Regge trajectories, viz.  $\text{Im} \lambda_n(E)$  versus  $\text{Re} \lambda_n(E)$  ( $\lambda_n(E)$  is the CAM). These probe electron attachment at the fundamental level near threshold, thereby allowing for the determination of reliable anionic binding energies (BEs). For the fullerene molecules,  $C_{20}$  through  $C_{92}$ , these BEs matched excellently with the measured EAs (see [11,12]). Thylwe [25] investigated Regge trajectories using the ABF potential, and demonstrated that for the Xe atom the Dirac Relativistic and non-Relativistic Regge trajectories yielded essentially the same  $\text{Re} \lambda_n(E)$  when the  $\text{Im} \lambda_n(E)$  was still very small. This clearly demonstrated the insignificant difference between the Relativistic and non-Relativistic calculations near the threshold electron impact energies, provided that the appropriate physics is accounted for adequately,

as in our case. Importantly, for the physical resonances the poles must be close to the real axis, namely  $\text{Im } \lambda_n(E) \ll 1$ .

The potential (2) has been used successfully with the appropriate values of  $\alpha$  and  $\beta$ . It was found that when the TCS, as a function of  $\beta$ , has a resonance [24] corresponding to the formation of a stable negative ion, this resonance lives the longest for a given value of the energy, which corresponds to the EA of the system (for ground state collisions) or the BE of the metastable/excited anion. This was found to be the case for all the systems, including fullerenes that we investigated thus far. This fixes the optimal value of “ $\beta$ ” in Equation (2) when the optimum value of  $\alpha = 0.2$ . The effective use of  $\text{Im } \lambda \rightarrow 0$  is demonstrated in [24] and carefully explained in [35]. Although we previously referred to Connor [36] for the physical interpretation of  $\text{Im } \lambda(E)$ , the original interpretation was given by Regge himself [37]. For a true bound state, namely  $E < 0$ ,  $\text{Im } \lambda(E) = 0$ , and therefore the angular life,  $1/(\text{Im } \lambda(E)) \rightarrow \infty$  implies that the system can never decay. Obviously, in our calculations  $\text{Im } \lambda(E)$  is not identical to zero, but this can be clearly seen in the Figures [35]; the dramatically sharp (long-lived) resonances hardly have a width, as opposed to shape resonances for instance (see also [24] for comparison). We limit the calculations of the TCSs to the near threshold energy region, namely below any excitation thresholds to avoid their effects.

We emphasize here that the investigation of the Regge trajectories allows us to readily identify the electron impact energy range where Relativity is unimportant in the calculation of the TCSs, i.e., for small-electron impact energies. Additionally, the use of the  $\text{Im } \lambda_n(E)$  allows us to differentiate among the important ground and metastable negative ion formation, as well as the shape resonances. The very small value of  $\text{Im } \lambda_n(E)$  indicates the presence of a ground state negative-ion formation, see for example [24].

### 3. Results

The focus of this paper is toward a fundamental understanding of negative-ion formation in low-energy electron scattering from the actinide atoms, Am, Cm, Bk, Es, No and Lr, through the calculation of electron elastic TCSs using the rigorous Regge pole method. From the characteristic dramatically sharp resonances in the TCSs manifesting ground, metastable and excited-state negative-ion formation, we extract the BEs of the formed negative ions during the collisions. These BEs, presented in Table 1, are used to understand the existing EAs of these atoms. The results are also used to explain the new manifestations in the near threshold TCSs of Am through Lr, as well as to elucidate the observed fullerene behavior in these TCSs. To strengthen the discussions of the results and the attendant conclusions, the standard measured EAs of the Au, Pt and At atoms are also presented, as well as the relevant data of the  $C_{60}$ ,  $C_{28}$ , and  $C_{24}$  fullerenes.

The calculated electron elastic TCSs for Am, Cm, Bk, Es, No and Lr atoms are presented in Figures 1–6, respectively. Indeed, generally all the TCSs in Figures are characterized by R-T minima, shape resonances (SRs) and dramatically sharp resonances, corresponding to the  $\text{Am}^-$ ,  $\text{Cm}^-$ ,  $\text{Bk}^-$ ,  $\text{Es}^-$ ,  $\text{No}^-$  and  $\text{Lr}^-$  anionic formation in their ground, metastable and excited states. Consequently, the need for their delineation and identification is evident so that the unambiguous and reliable determination of the atoms' EAs can be achieved. At a glance, the TCSs for each atom in the Figures appear complicated. However, they are readily understood and interpreted if we focus on one single color-coded curve at a time, since they represent the scattering from different states, resulting in negative-ion formation. For the convenience of analysis, the TCSs in the Figures are divided into two groups: Group 1 consists of the TCSs of Am, Cm and Bk, while Group 2 has TCSs for Es, No and Lr. Group 1 is characterized by the appearance of the polarization-induced metastable TCS with a deep R-T minimum near threshold. In Group 2 TCSs this R-T minimum has flipped over to a SR very close to threshold. The second metastable TCS (blue curve) changes very little throughout the Figures; here we are interested only in the BE of its anion.

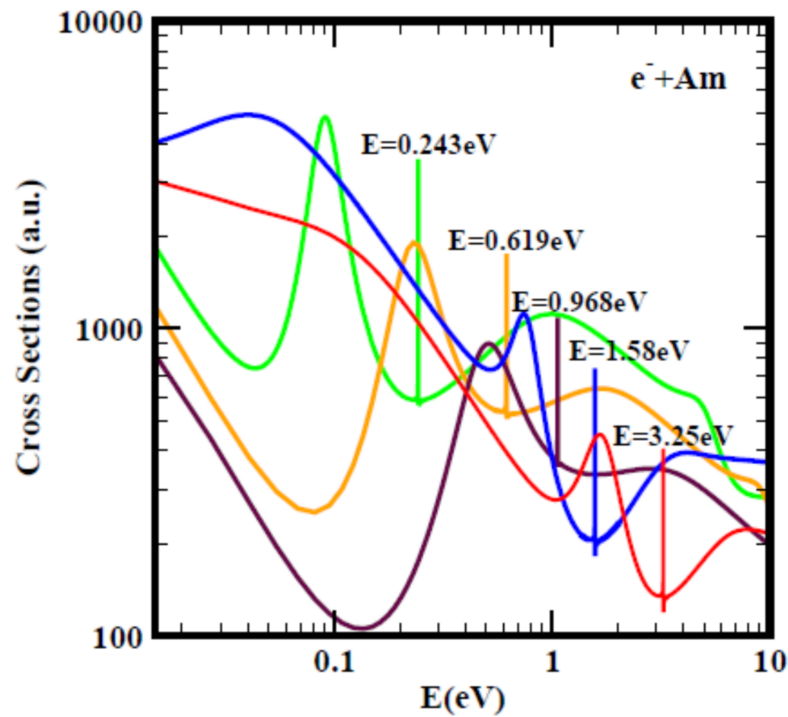


**Figure 1.** Total cross sections (a.u) for electron–Am scattering. Red, blue and brown curves represent ground and metastable TCSs, respectively. Orange and green curves are two excited-state TCSs. The polarization-induced TCS due to size effect is the brown curve.

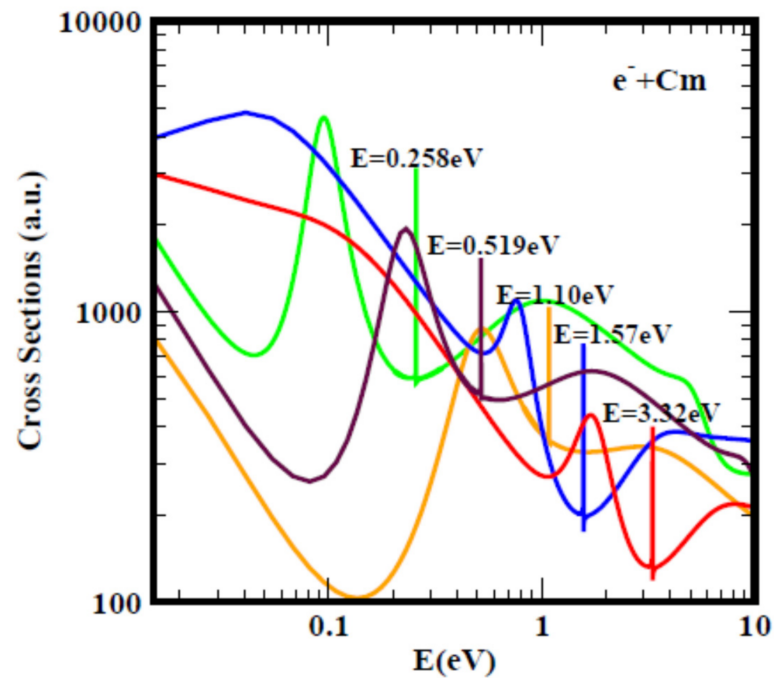


**Figure 2.** Total cross sections (a.u) for electron–Cm scattering. Red, blue and orange curves represent ground and metastable TCSs, respectively. Brown and green curves are two excited-state TCSs. The polarization-induced TCS due to size effect is the orange curve.

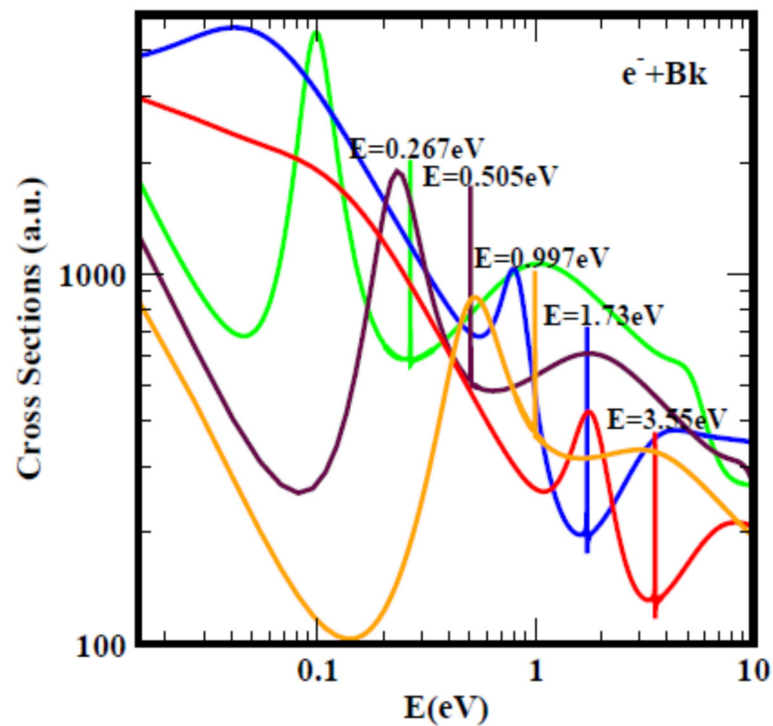


**Figure 3.** Total cross sections (a.u) for electron–Bk scattering. Red, blue and orange curves represent ground and metastable TCSs, respectively. Brown and green curves are two excited-state TCSs. The orange curve is the polarization-induced TCS due to size effect.

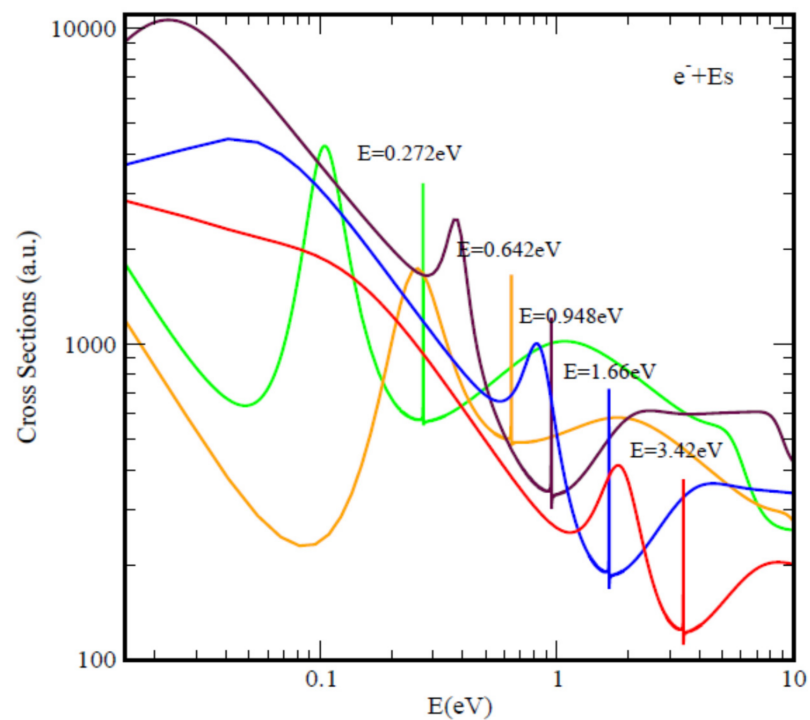


**Figure 4.** Total cross sections (a.u) for electron–Es scattering. Red, blue and brown curves represent, ground and metastable TCSs, respectively. Orange and green curves are two excited-state TCSs. The polarization-induced TCS due to size effect is the brown curve.

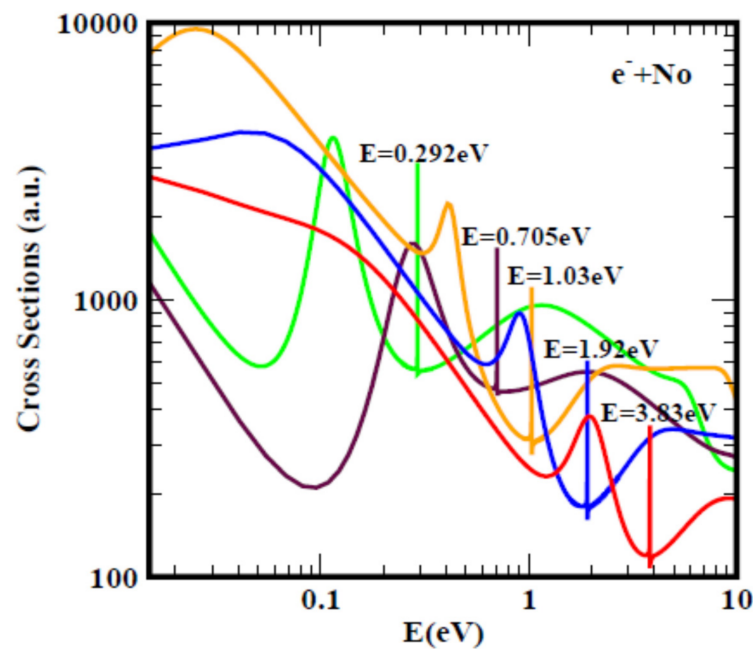


**Figure 5.** Total cross sections (a.u) for electron–No scattering. Red, blue and orange curves represent, ground and metastable TCSs, respectively. Brown and green curves are two excited-state TCSs. The polarization-induced TCS due to size effect is the orange curve.

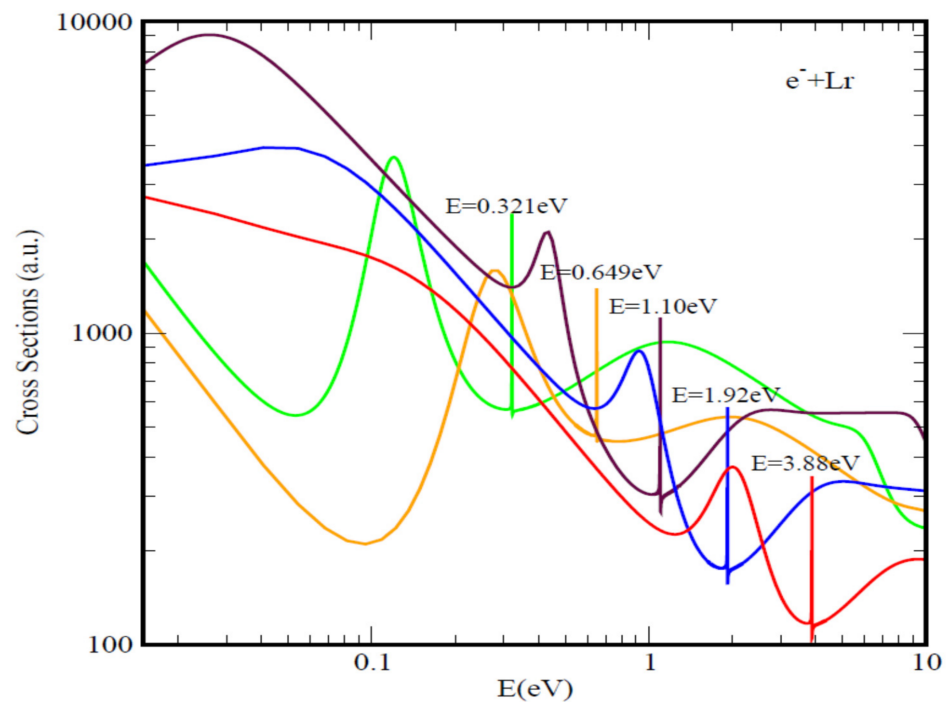


**Figure 6.** Total cross sections (a.u) for electron–Lr scattering. Red, blue and brown curves represent, ground and metastable TCSs, respectively. Orange and green curves are two excited-state TCSs. The polarization-induced TCS due to size effect is represented by the brown curve.

Figure 1 displays the TCSs for atomic Am; they typify those of the other actinides. Three general observations can be made: (1) The ground-state TCS (red curve) with the anionic B,E located at the second R-T minimum, is typical of complex heavy atoms such as Au, Pt and At; (2) The highest excited-state TCS (green curve) exhibits fullerene behavior [11]; (3) The metastable TCS (brown curve), with a deep R-T minimum, represents the

polarization-induced TCS. It manifests the combined effects (size and 6d-orbital collapse), significantly impacting the polarization interaction, thereby causing this first appearance of the polarization-induced TCS in the actinide atoms, viz. in Pu [7]. Below, we discuss the individual results for clarity.

### 3.1. Ground State Total Cross Sections (TCSs)

The fundamental physics underlying these curves can be readily understood if we focus on each color-coded TCS. For the analysis we select the ground-state TCS curve, the red curve of Figure 1. From the near threshold the ground-state TCS decreases monotonically with the increase in the electron impact energy,  $E$ . As the electron continues to approach the Am atom in its ground state, the atom becomes polarized, reaching a maximum polarization manifested through the appearance of the first R-T minimum in the TCS at about 1.1 eV. With a further increase in  $E$ , the electron becomes trapped by the centrifugal barrier whose effect is seen through the appearance of the SR at about 1.6 eV. As the electron continues to leak out of the barrier, the polarizability of the Am atom leads to the generation of the second deep R-T minimum at 3.28 eV. At this absolute minimum, the long-lived ground state  $\text{Am}^-$  anion is formed; its BE is seen to be 3.32 eV, corresponding to the EA of the atomic Am, consistent with the Au, Pt and At cases, including the fullerene molecules. At this R-T minimum, the Am atom is transparent to the incident electron, and the electron becomes attached to it forming the stable  $\text{Am}^-$  ground state anion. The electron completes many angular rotations about the Am atom as the  $\text{Am}^-$  anion decays, with the angular lifetime determined by  $1/(\text{Im}\lambda(E)) \rightarrow \infty$ , since for the ground-state anionic formation,  $\text{Im}\lambda(E) \rightarrow 0$ . Indeed, the appearance of the R-T minimum in the TCSs of Figure 1, demonstrating the vital importance of the electron correlation effects and the polarization interaction, corroborates that these effects are accounted for adequately in our calculation, consistent with the conclusion of [38].

### 3.2. Polarization-Induced Total Cross Sections (TCSs)

We now consider the polarization-induced TCSs appearing in the TCSs of Figure 1 (brown curve), Figure 2 (orange curve) and Figure 3 (orange curve). Such a TCS first appeared in the actinide TCSs of Pu (see Figure 4 of [7]). This is due to the size effect and the first collapse of the 6d-orbital in transitioning from  $\text{Np}[\text{Rn}]7s^25f^46d$  to  $\text{Pu}[\text{Rn}]7s^25f^6$ . This also causes the ground state BE of  $\text{Pu}^-$  to increase to 3.25 eV. The combined effects (size and 6d-orbital collapse) impact the polarization interaction significantly, causing the first appearance of the polarization-induced TCS in the actinide atoms, namely in Pu. The polarization-induced TCSs in the Am, Cm and Bk can be explained similarly. It is noted here that the ground-state BEs of the  $\text{Pu}^-$  and  $\text{Am}^-$  anions are the same: 3.25 eV. However, the BE of the ground-state  $\text{Cm}^-$  anion increases to 3.32 eV due to the size effect.

In Figure 1, there are two metastable TCSs, namely the blue and the brown curves. The blue curve, also a polarization-induced TCS, does not change significantly as we move from Am through Lr. In all these atoms, the very sharp resonance in the second R-T minimum of the blue curve with a slight maximum near the threshold always remains behind the SR of the ground state curve. However, in the TCSs for fullerenes, the sharp resonance moves closer to the ground state resonance as the fullerene size increases. (See comparisons in Figures 1 and 2 of [39]).

In the Group 2 TCSs, namely for Es, No and Lr (Figures 4–6) the deep R-T minimum flips over to an SR very close to the threshold. This is explained through the second collapse of the 6d-orbital, in transitioning from  $\text{Cm}[\text{Rn}]7s^25f^76d$  to  $\text{Bk}[\text{Rn}]7s^25f^9$ . The impact of this on the polarization interaction is to flip the deep R-T minimum into an SR very close to the threshold and increase the ground state BE of the  $\text{Bk}^-$  anion significantly, to 3.55 eV (this can be compared with those of the  $\text{Cm}^-$  and  $\text{Es}^-$  ground-state BE values of 3.32 eV and 3.42 eV, respectively).

### 3.3. Fullerene Molecular Behavior

In the paper [11] it was concluded that the TCSs for  $C_{20}$  fullerene exhibited atomic behavior while those for  $C_{112}$  demonstrated a strong departure from atomic behavior. This behavior was attributed to the size effect, which impacted the polarization interaction significantly as the fullerene increased in size. The value of the first excited-state TCS at the second R-T minimum divided by that of the TCS at the first R-T minimum, defined the ratio  $R$ . It was used in the analysis as the fullerene size varied from  $C_{20}$  (the smallest fullerene thought to exist at that time) through to  $C_{112}$ . The conclusion was that for  $R < 1$ , fullerene behavior was implied (as an example,  $R < 1$  for  $C_{112}$ ) while for  $R > 1$ , such as in the TCSs for atomic Au and At, the behavior was atomic. In Table 1, the ratio  $R$  is also included to demonstrate that most of the TCSs for the actinides exhibited fullerene behavior. The ratio was obtained using the highest excited-state TCSs (the green curves in Figures 1–6) [11]. For clarity, we also included this ratio  $R$  for the fullerenes  $C_{60}(0.24)$ ,  $C_{28}(0.66)$ , and  $C_{24}(1.05)$ . Clearly, it increases as the size of the fullerene approaches that of the atom; see the ratios for Au and Lr. The  $C_{28}$  and  $C_{24}$  fullerenes were selected because the measured EAs of  $C_{28}$  [40,41] and  $C_{24}$  [40,41] agreed well with the Regge pole calculated BEs, see Table 1.

Indeed, the results demonstrated the crucial importance of the polarization interaction in low-energy electron scattering calculations of TCSs of complex, heavy, multi-electron systems. These characteristic R-T minima were also observed in the Dirac R-matrix low-energy electron elastic scattering cross sections calculations for the heavy, alkali-metal atoms Rb, Cs and Fr [42], corroborated that the important polarization interaction was accounted for adequately in our calculation, consistent with the conclusion by Johnson and Guet [38]. The energy positions of the sharp resonances correspond to the anionic BEs of the formed negative ions during the electron collision with the ground, metastable and excited actinide atoms. The data from Figures 1–6 are summarized in Table 1. The anionic BEs for the ground, metastable and excited  $Am^-$  through  $Lr^-$  negative ions are compared with the Relativistic Configuration-Interaction (RCI) [43] and the QR-LSD-GX-SIC-GWB [44]-calculated EAs.

### 3.4. Understanding Table 1

To better understand and appreciate the results of our investigation in the context of the available EAs of the actinide atoms, Am through Lr, we included in Table 1 the standard measured EAs of the Au, Pt and At atoms, as well as of the  $C_{60}$  fullerene molecule. These were compared with our Regge-pole-calculated BEs of their ground-state negative ions and the agreement was excellent. Notably, each of these atoms (Au, Pt and At) has, in addition to the ground-state anionic BE, a metastable and an excited-state anionic BE. A similar behavior is also exhibited by the Regge-pole-calculated anionic BEs of the Th atom (see also Ref. [7]). However, for Th there are two anionic excited states with BEs (EXT-1 0.149 eV and EXT-2 0.549 eV), including a ground-state anionic BE of 3.09 eV and two metastable anionic BEs of 0.905 eV and 1.36 eV. The measured and calculated EAs of Th are 0.608 eV and 0.599 eV [5], respectively. Both these values are closer to our excited-state BE and not to the ground-state value.

We now analyze the data in Table 1 for the actinide atoms from Am through Lr in the context of the calculated EAs [43,44]; there are no measured EAs available for these atoms for a comparison. We first observe that, due to the size effect, each of these atoms has a ground-state anionic BE, two metastable anionic BEs (MS-1 and MS-2) and two excited-state anionic BEs (EXT-1 and EXT-2), see Table 1. Their ground state anionic BEs lie between 3.25 eV and 3.88 eV; they generally increase according to the size of the atom. The RCI [43] and GW [44]-calculated EAs of these atoms are presented in the last two columns, respectively. A quick glance at the values shows that they vary significantly from each other. Even worse are the GW [44] EAs, which have both positive and negative values, making it very difficult to interpret their meaning. Notwithstanding, we attempted to compare and contrast the EAs of [43,44] with our Regge-pole calculated anionic BEs; the closest are those labeled EXT-1 and EXT-2.

For the Am atom the EAs of [43,44] are small compared with our anionic BEs of the excited states, EXT-1 (0.243 eV) and EXT-2 (0.619 eV) to carry out a meaningful comparison. For atomic Cm the EA of 0.321 eV [43] is close to the 0.283 eV of [44] as well as to our anionic BE value of 0.258 eV. However, the 0.447 eV EA of [44] is closer to our BE value of 0.519 eV. Here it is simple to conclude that the EAs of [43,44] correspond to the BE of an excited anionic state of Cm. Our BE values of 0.267 eV and 0.505 eV for the Bk- anion are close to the Abs (−0.276) eV and Abs (−0.503) eV EA values of [44], respectively. However, they are larger than the 0.085 eV EA of [43]. Clearly, it is challenging to draw a definitive conclusion from these data. For the EA of Es, a fair comparison between the values of [43,44] cannot be made with respect to our BEs because of the significant differences between the EAs. There is no EA value from [43] for No. Our anionic BE of 0.292 eV cannot be compared with the very large negative values of [44]. For atomic Lr our anionic BE values of 0.321 eV and 0.649 eV are reasonably close to the EAs of 0.295 eV and 0.465 eV of [43], respectively. It is noted here that there is a SR at 0.43 eV (between 0.321 eV and 0.649 eV, see also Figure 6). Our first excited state BE value of 0.321 eV is close to the Abs (−0.313) eV EA of [44]. Additionally, the EA value of 0.310 eV [45] is very close to our BE value of 0.321 eV, while the 0.476 eV EA value of [46] could be used safely for the anionic BE of the first excited state or the second excited state. Also included in Table 1 for comparisons are the theoretical BEs of Au [47] and Pt [47] as well as the EAs of At [48–50], C<sub>28</sub> [51] and C<sub>24</sub> [52].

Clearly, the analysis leaves one much confused regarding the meaning of the EAs of the actinide atoms as was the case with the lanthanide atoms [8]. Indeed, the sophisticated theoretical methods experience difficulties producing unambiguous and reliable EAs of the actinide atoms. This calls for careful theoretical investigation of the EA of each actinide atom as was done for the case of the At atom [4].

From the comparisons in Table 1 we can safely conclude:

- (1) The measured and calculated EAs of Th [5] are quite close to the Regge-pole-calculated, second, excited-state, anionic BE and not to the ground-state, anionic BE, as was found in the cases of the Au, Pt and At atoms, as well as the C<sub>60</sub> fullerene molecule. Indeed, these EAs could be considered at best as the BEs of excited states of the formed negative ions, but definitely not with the ground state.
- (2) The existing EAs of the Lr atom calculated using the sophisticated theoretical methods [43–45] tend to be reasonably close to the Regge-pole BE of the first excited anionic state. The second set of the EAs of [43,45] are closer to the Regge pole BE of the second excited anionic state. These EAs could be used to guide future experimental research and the theoretical exploration of the EA of Lr.

Indeed, the serious question still remains: does the EA of complex heavy systems such as the actinides correspond to the BE of electron attachment in the ground or the excited state of the formed anion during the collision?

**Table 1.** Negative ion binding energies (BEs) in eV and energy positions of ground-state Ramsauer–Townsend (R-T) minima, in eV obtained from the TCSs for the atoms Am, Cm, Bk, Es, No and Lr. Additionally, included for comparison are the data for Au, Pt, At, Th and Pu, as well as for C<sub>60</sub> fullerene. GRS, MS-*n* and EXT-*n* (*n* = 1, 2) represent ground, metastable and excited states, respectively. The experimental EAs, EXPT and the theoretical EAs, including RCI [43] and GW [44], are also presented. R is the ratio described in the text.

System/ Z	BEs GRS	BEs MS-1	BEs MS-2	EAs EXPT	BEs EXT-1	BEs EXT-2	R-T GRS	BEs/EAs Theory	EAs [43]	EAs [44]	R
Au 79	2.26	0.832	-	2.309 [13] 2.301 [14] 2.306 [15]	0.326	-	2.24	2.262 [47]	-	-	1.36
C <sub>60</sub>	2.66	1.86	1.23	2.684 [18] 2.666 [19]	0.203	0.378	2.67	2.66 [12]	-	-	0.24
At 85	2.41	0.918	-	2.416 [3]	0.412	-	-	2.38 [4] 2.42 [48] 2.51 [49] 2.80 [50]	-	-	-
Pt 78	2.16	1.197	-	2.128 [13] 2.125 [16] 2.123 [17]	0.136	-	-	2.163 [47]	-	-	-
C <sub>28</sub>	3.10	1.80	0.305	2.80 [40] 3.00 [41]	-	-	2.97	3.39 [51]	-	-	0.66
C <sub>24</sub>	3.79	2.29	0.428	3.75 [40] 2.90 [41]	-	-	3.71	3.55 [52]	-	-	1.06
Th 90	3.09	1.36	0.905	0.608 [5]	0.149	0.549	3.10	0.599 [5]	0.368	1.17	-
Pu 94	3.25	1.57	1.22	N/A	0.225	0.527	-	-	0.085	-0.503 -0.276	0.72
Am 95	3.25	1.58	0.968	N/A	0.243	0.619	3.27	-	0.076	0.103	0.78
Cm 96	3.32	1.57	1.10	N/A	0.258	0.519	3.31	-	0.321	0.283 0.449	0.83
Bk 97	3.55	1.73	0.997	N/A	0.267	0.505	3.53	-	0.031	-0.503 -0.276	0.86
Es 99	3.42	1.66	0.948	N/A	0.272	0.642	3.44	-	0.002	0.103 0.142	0.87
No 102	3.83	1.92	1.03	N/A	0.292	0.705	3.85	-	-	-2.302 -2.325	0.94
Lr 103	3.88	1.92	1.10	N/A	0.321	0.649	3.90	0.310 [45] 0.160 [45] 0.476 [46]	0.465 0.295	-0.212 -0.313	1.05

#### 4. Summary and Conclusions

In this paper we investigated the response of the actinide atoms Am, Cm, Bk, Es, No and Lr, to low-energy electron collisions through the elastic TCSs calculation using our robust Regge-pole method. The objective was to obtain first-time electron elastic TCSs and extract unambiguous and reliable anionic binding energies. The TCSs for the investigated atoms were found to be characterized generally by ground, metastable and excited negative-ion formations, shape resonances and R-T minima. The anionic BEs extracted from the TCSs were compared with the existing EAs. Except for Th the experimental EAs for the actinides were unavailable because of the difficulty of handling them experimentally due to their radioactive nature.

We also discovered new manifestations in the low-energy electron scattering TCSs of the atoms. Namely, we discovered both the atomic and fullerene molecular behavior near

the threshold and also a polarization-induced metastable cross section with a deep R-T minimum near the threshold of the Am, Cm and Bk TCSs. In the TCSs for Es, No and Lr, this R-T minimum flipped over to a shape resonance appearing very close to the threshold. We attributed these peculiar tunable behaviors in the TCSs to both size effects and the 6d-orbital collapse, significantly impacting the polarization interaction. This provided a novel mechanism of tuning a shape resonance and an R-T minimum through the polarization interaction via the size effect. The comparison between the Regge-pole-calculated anionic BEs with the existing theoretical EAs demonstrated that the existing theoretical calculations tended to obtain the excited-states BEs and equate them with the EAs (this was also found with the lanthanide atoms [8]).

We conclude that the meaning of the existing calculated and/or measured EAs of the actinide atoms is both ambiguous and confusing because these EAs are close to the Regge-pole-calculated BEs of excited anionic states (see Table 1). This conflicts directly with the usual meaning of the EAs found in the measurements of the EAs of atomic Au, Pt and At, as well as of the fullerene molecules, C<sub>20</sub> through C<sub>92</sub>. For these heavy, complex electron systems, their EAs matched excellently with the Regge-pole-calculated, ground-state anionic BEs. The ground, metastable and excited negative-ion BEs calculated here for the actinide atoms, and presented in [8] for the lanthanide atoms, can now be used in sophisticated theoretical methods such as the Coupled-Cluster method, Dirac R-matrix, MCDHF, and MCDHF-RCI, etc., to generate reliable EAs for the actinide atoms, wave functions and fine-structure energies. What is needed for the unambiguous and definitive meaning of the EAs of the actinide atoms is to use our anionic BEs in sophisticated theoretical methods and carry out careful investigations, such as those conducted in [3,4], for the At atom.

**Author Contributions:** Z.F. and A.Z.M. are responsible for the conceptualization, methodology, investigation, formal analysis and writing of the original draft, as well as rewriting and editing. A.Z.M. is also responsible for securing the funding for the research. All authors have read and agreed to the published version of the manuscript.

**Funding:** Research was supported by the U.S. DOE, Division of Chemical Sciences, Geosciences and Biosciences, Office of Basic Energy Sciences, Office of Energy Research, Grant: DE-FG02-97ER14743.

**Acknowledgments:** Research was supported by the U.S. DOE, Division of Chemical Sciences, Geosciences and Biosciences, Office of Basic Energy Sciences, Office of Energy Research, Grant: DE-FG02-97ER14743. The computing facilities of National Energy Research Scientific Computing Center, also funded by U.S. DOE are greatly appreciated.

**Conflicts of Interest:** The authors declare no conflict of interest or state.

## References

1. Kasdan, K.; Lineberger, W.C. Alkali-metal negative ions. II. Laser photoelectron spectrometry. *Phys. Rev. A* **1974**, *10*, 1658. [[CrossRef](#)]
2. Cheng, S.-B.; Castleman, A.W. Direct experimental observation of weakly-bound character of the attached electron in europium anion. *Sci. Rep.* **2015**, *5*, 12414. [[CrossRef](#)]
3. Leimbach, D.; Karls, J.; Guo, Y.; Ahmed, R.; Ballof, J.; Bengtsson, L.; Pamies, F.B.; Borschevsky, A.; Chrysalidis, K.; Eliav, E.; et al. The electron affinity of astatine. *Nat. Commun.* **2020**, *11*, 3824. [[CrossRef](#)]
4. Si, R.; Froese Fischer, C. Electron affinities of At and its homologous elements Cl, Br, I. *Phys. Rev. A* **2018**, *98*, 052504. [[CrossRef](#)]
5. Tang, R.; Si, R.; Fei, Z.; Fu, X.; Lu, Y.; Brage, T.; Liu, H.; Chen, C.; Ning, C. Candidate for Laser Cooling of a Negative Ion: High-Resolution Photoelectron Imaging of Th<sup>-</sup>. *Phys. Rev. Lett.* **2019**, *123*, 203002. [[CrossRef](#)]
6. Tang, R.; Chen, X.; Fu, X.; Wang, H.; Ning, C. Electron affinity of the hafnium atom. *Phys. Rev. A* **2018**, *98*, 020501. [[CrossRef](#)]
7. Felfli, Z.; Msezane, A.Z. Negative Ion Formation in Low-Energy Electron Collisions with the Actinide Atoms Th, Pa, U, Np and Pu. *Appl. Phys. Res.* **2019**, *11*, 52. [[CrossRef](#)]
8. Felfli, Z.; Msezane, A.Z. Low-Energy Electron Elastic Total Cross Sections for Ho, Er, Tm, Yb, Lu, and Hf Atoms. *Atoms* **2020**, *8*, 17. [[CrossRef](#)]
9. Felfli, Z.; Msezane, A.Z.J. Conundrum in Measured Electron Affinities of Complex Heavy Atoms. *J. At. Mol. Condens. Nano Phys.* **2018**, *5*, 73. [[CrossRef](#)]

10. Ciborowski, S.M.; Liu, G.; Blankenhorn, M.; Harris, R.M.; Marshall, M.A.; Zhu, Z.; Bowen, K.H.; Peterson, K.A. The electron affinity of the uranium atom. *J. Chem. Phys.* **2021**, *154*, 224307. [[CrossRef](#)]
11. Msezane, A.Z.; Felfli, Z. New insights in low-energy electron-fullerene interactions. *Chem. Phys.* **2018**, *503*, 50. [[CrossRef](#)]
12. Felfli, Z.; Msezane, A.Z. Simple method for determining fullerene negative ion formation. *Eur. Phys. J. D* **2018**, *72*, 78. [[CrossRef](#)]
13. Hotop, H.; Lineberger, W.C. Dye-laser photodetachment studies of Au<sup>-</sup>, Pt<sup>-</sup>, PtN<sup>-</sup>, and Ag<sup>-</sup>. *J. Chem. Phys.* **2003**, *58*, 2379. [[CrossRef](#)]
14. Andersen, T.; Haugen, H.K.; Hotop, H. Binding Energies in Atomic Negative Ions: III. *J. Phys. Chem. Ref. Data* **1999**, *28*, 1511. [[CrossRef](#)]
15. Zheng, W.; Li, X.; Eustis, S.; Grubisic, A.; Thomas, O.; De Clercq, H.; Bowen, K. Anion photoelectron spectroscopy of Au–(H<sub>2</sub>O) 1, 2, Au<sub>2</sub>–(D<sub>2</sub>O) 1–4, and AuOH<sup>-</sup>. *Chem. Phys. Lett.* **2007**, *444*, 232–236. [[CrossRef](#)]
16. Bilodeau, R.C.; Scheer, M.; Haugen, H.K.; Brooks, R.L. Near-threshold laser spectroscopy of iridium and platinum negative ions: Electron affinities and the threshold law. *Phys. Rev. A* **1999**, *61*, 012505. [[CrossRef](#)]
17. Gibson, D.; Davies, B.J.; Larson, D.J. The electron affinity of platinum. *J. Chem. Phys.* **1993**, *98*, 5104. [[CrossRef](#)]
18. Huang, D.-L.; Dau, P.D.; Liu, H.T.; Wang, L.-S. High-resolution photoelectron imaging of cold C<sub>60</sub><sup>-</sup> anions and accurate determination of the electron affinity of C<sub>60</sub>. *J. Chem. Phys.* **2014**, *140*, 224315. [[CrossRef](#)] [[PubMed](#)]
19. Brink, C.; Andersen, L.H.; Hvelplund, P.; Mathur, D.; Voldstad, J.D. Laser photodetachment of C<sub>60</sub><sup>-</sup> and C<sub>70</sub><sup>-</sup> ions cooled in a storage ring. *Chem. Phys. Lett.* **1995**, *233*, 52–56. [[CrossRef](#)]
20. Frautschi, S.C. *Regge Poles and S-Matrix Theory*; Benjamin: New York, NY, USA, 1963; Chapter X.
21. D’Alfaro, V.; Regge, T.E. *Potential Scattering*; North-Holland: Amsterdam, The Netherlands, 1965.
22. Omnes, R.; Froissart, M. *Mandelstam Theory and Regge Poles: An Introduction for Experimentalists*; Benjamin: New York, NY, USA, 1963; Chapter 2.
23. Hiscox, A.; Brown, B.M.; Marletta, M. On the low energy behavior of Regge poles. *J. Math. Phys.* **2010**, *51*, 102104. [[CrossRef](#)]
24. Felfli, Z.; Msezane, A.Z.; Sokolovski, D. Resonances in low-energy electron elastic cross sections for lanthanide atoms. *Phys. Rev. A* **2009**, *79*, 012714. [[CrossRef](#)]
25. Thylwe, K.W. On relativistic shifts of negative-ion resonances. *Eur. Phys. J. D* **2012**, *66*, 7. [[CrossRef](#)]
26. Mulholland, H.P. An asymptotic expansion for  $\Sigma(2n + 1)\exp(-\Lambda\sigma(n + 1/2)^2)$ . *Proc. Camb. Phil. Soc.* **1928**, *24*, 280–289. [[CrossRef](#)]
27. Macek, J.H.; Krstic, P.S.; Ovchinnikov, S.Y. Regge Oscillations in Integral Cross Sections for Proton Impact on Atomic Hydrogen. *Phys. Rev. Lett.* **2004**, *93*, 183203. [[CrossRef](#)]
28. Sokolovski, D.; Felfli, Z.; Ovchinnikov, S.Y.; Macek, J.H.; Msezane, A.Z. Regge oscillations in electron-atom elastic cross sections. *Phys. Rev. A* **2007**, *76*, 012705. [[CrossRef](#)]
29. Dolmatov, V.K.; Amusia, M.Y.; Chernysheva, L.V. Electron elastic scattering off A@C<sub>60</sub>: The role of atomic polarization under confinement. *Phys. Rev. A* **2017**, *95*, 012709. [[CrossRef](#)]
30. Felfli, Z.; Belov, S.; Avdonina, N.B.; Marletta, M.; Msezane, A.Z.; Naboko, S.N. In *Proceedings of the Third International Workshop on Contemporary Problems in Mathematical Physics, Cotonou, Republic of Benin, 1–7 November 2003*; Govaerts, J., Hounkonnou, M.N., Msezane, A.Z., Eds.; World Scientific: Singapore, 2004; pp. 218–232.
31. Belov, S.; Thylwe, K.-E.; Marletta, M.; Msezane, A.Z.; Naboko, S.N. On Regge pole trajectories for a rational function approximation of Thomas–Fermi potentials. *J. Phys. A* **2010**, *43*, 365301. [[CrossRef](#)]
32. Belov, S.M.; Avdonina, N.B.; Felfli, Z.; Marletta, M.; Msezane, A.Z.; Naboko, S.N. Semiclassical approach to Regge poles trajectories calculations for nonsingular potentials: Thomas–Fermi type. *J. Phys. A Math. Gen.* **2004**, *37*, 6943. [[CrossRef](#)]
33. Thylwe, K.-E.; McCabe, P. Partial-wave analysis of particular peaks in total scattering cross sections caused by a single partial wave. *Eur. Phys. J. D* **2014**, *68*, 323. [[CrossRef](#)]
34. Burke, P.G.; Tate, C. A program for calculating regge trajectories in potential scattering. *Comp. Phys. Commun.* **1969**, *1*, 97. [[CrossRef](#)]
35. Msezane, A.Z.; Felfli, Z. Low-energy electron scattering from fullerenes and heavy complex atoms: Negative ions formation. *Eur. Phys. J. D* **2018**, *72*, 173. [[CrossRef](#)]
36. Connor, J.N.L. New theoretical methods for molecular collisions: The complex angular-momentum approach. *J. Chem. Soc. Faraday Trans.* **1990**, *86*, 1627. [[CrossRef](#)]
37. Regge, T. Bound States, Shadow States and Mandelstam Representation. *Nuovo Cimento.* **1960**, *18*, 947. [[CrossRef](#)]
38. Johnson, W.R.; Guet, C. Elastic scattering of electrons from Xe, Cs<sup>+</sup>, and Ba<sub>2</sub><sup>+</sup>. *Phys. Rev. A* **1994**, *49*, 1041. [[CrossRef](#)] [[PubMed](#)]
39. Msezane, A.Z. Negative Ion Binding Energies in Complex Heavy Systems. *JAMCNP* **2018**, *5*, 195–204. [[CrossRef](#)]
40. Achiba, Y.; Kohno, M.; Ohara, M.; Suzuki, S.; Shiromaru, H.J. Electron detachment spectroscopic study on carbon and silicon cluster anions. *J. Electron. Spectros. Rel. Phenom.* **2005**, *142*, 231. [[CrossRef](#)]
41. Yang, S.; Taylor, K.J.; Craycraft, M.J.; Conceicao, J.; Pettiette, C.L.; Cherhovsky, O.; Smalley, R.E. UPS of 2–30-atom carbon clusters: Chains and rings. *Chem. Phys. Lett.* **1988**, *144*, 431. [[CrossRef](#)]
42. Bahrim, C.; Thumm, U. Low-lying <sup>3</sup>P<sup>o</sup> and <sup>3</sup>S<sup>e</sup> states of Rb<sup>-</sup>, Cs<sup>-</sup>, and Fr<sup>-</sup>. *Phys. Rev. A* **2000**, *61*, 022722. [[CrossRef](#)]
43. O’Malley, S.M.; Beck, D.R. Valence calculations of actinide anion binding energies: All bound 7p and 7s attachments. *Phys. Rev. A* **2009**, *80*, 032514. [[CrossRef](#)]
44. Guo, Y.; Whitehead, M.A. Electron affinities of alkaline-earth and actinide elements calculated with the local-spin-density-functional theory. *Phys. Rev. A* **1989**, *40*, 28. [[CrossRef](#)]

45. Eliav, E.; Kaldor, U.; Ishikawa, Y. Transition energies of ytterbium, lutetium, and lawrencium by the relativistic coupled-cluster method. *Phys. Rev. A* **1995**, *52*, 291. [[CrossRef](#)] [[PubMed](#)]
46. Borschevsky, A.; Eliav, E.; Vilkas, M.J.; Ishikawa, Y.; Kaldor, U. Transition energies of atomic lawrencium. *Eur. Phys. J. D* **2007**, *45*, 115–119. [[CrossRef](#)]
47. Msezane, A.Z.; Felfli, Z.; Sokolovski, D. Near-threshold resonances in electron elastic scattering cross sections for Au and Pt atoms: Identification of electron affinities. *J. Phys. B At. Mol. Opt. Phys.* **2008**, *41*, 105201. [[CrossRef](#)]
48. Li, J.; Zhao, Z.; Andersson, M.; Zhang, X.; Chen, C. Theoretical study for the electron affinities of negative ions with the MCDHF method. *J. Phys. B* **2012**, *45*, 165004. [[CrossRef](#)]
49. Felfli, Z.; Msezane, A.Z.; Sokolovski, D. Slow electron elastic scattering cross sections for In, Tl, Ga and At atoms. *J. Phys. B At. Mol. Opt. Phys.* **2012**, *45*, 045201. [[CrossRef](#)]
50. Zollweg, R.J. Electron Affinities of the Heavy Elements. *J. Chem. Phys.* **1969**, *50*, 4251. [[CrossRef](#)]
51. Munoz-Castro, R.A. Bruce King. *J. Comput. Chem.* **2016**, *38*, 44. [[CrossRef](#)]
52. Tiago, M.L.; Kent, P.R.C.; Hood, R.Q.; Reboledo, F. A Neutral and charged excitations in carbon fullerenes from first-principles many-body theories. *J. Chem. Phys.* **2008**, *129*, 084311. [[CrossRef](#)]